THE JOURNAL OF BIOLOGICAL CHEMISTRY VOL. 285, NO. 31, pp. 23994–24002, July 30, 2010
Printed in the U.S.A.

Differences in the Large Extracellular Loop between the K^+-Cl^- Cotransporters KCC2 and KCC4*[S]

Received for publication, May 12, 2010 Published, JBC Papers in Press, June 1, 2010, DOI 10.1074/jbc.M110.144063

Anna-Maria Hartmann[‡], Meike Wenz[§], Adriana Mercado[¶], Christof Störger[§1], David B. Mount[¶‖], Eckhard Friauf[§], and Hans Gerd Nothwang[‡§2]

From the [‡]Department of Neurogenetics, Institute for Biology and Environmental Sciences, Carl von Ossietzky University, Carl von Ossietzky Strasse 9-11, 26129 Oldenburg, Germany, the [§]Animal Physiology Group, Department of Biology, University of Kaiserlautern, Erwin-Schrödinger Strasse 13, 67663 Kaiserslautern, Germany, the [¶]Renal Division, Brigham and Women's Hospital, Harvard Medical School, Boston, Massachusetts 02115, and the [‖]Renal Division, Veterans Affairs Boston Healthcare System, West Roxbury, Massachusetts 02132

K^+Cl^- cotransporters (KCCs) play fundamental physiological roles in processes such as inhibitory neurotransmission and cell volume regulation. Mammalian genomes encode four distinct KCC paralogs, which share basic transport characteristics but differ significantly in ion affinity, pharmacology, and relative sensitivity to cell volume. Studies to identify divergence in functional characteristics have thus far focused on the cytoplasmic termini. Here, we investigated sequence requirements of the large extracellular loop (LEL) for function in KCC2 and KCC4. Mutation of all four evolutionarily conserved cysteines abolished KCC2 transport activity. This behavior differs from that of its closest relative, KCC4, which is insensitive to this mutation. Chimeras supported the differences in the LEL of the two cotransporters, because swapping wild-type LEL resulted in functional KCC2 but rendered KCC4 inactive. Insertion of the quadruple cysteine substitution mutant of the KCC4 loop, which was functional in the parental isoform, abolished transport activity in KCC2. Dose-response curves of wild-type and chimeric KCCs revealed that the LEL contributes to the different sensitivity to loop diuretics; a KCC2 chimera containing the KCC4 LEL displayed an IC_{50} of 396.5 μM for furosemide, which was closer to KCC4 (548.8 μM) than to KCC2 (184.4 μM). Cell surface labeling and immunocytochemistry indicated that mutations do not affect trafficking to the plasma membrane. Taken together, our results show a dramatic and unexpected difference in the sequence requirements of the LEL between the closely related KCC2 and KCC4. Furthermore, they demonstrate that evolutionarily highly conserved amino acids can have different functions within KCC members.

K^+-Cl^- cotransporters (KCCs)[3] mediate the electroneutral transport of K^+ and Cl^- across the plasma membrane. In mammals, the family consists of the four members KCC1 - KCC4, which are involved in different fundamental physiological processes. KCC2 is essential for the hyperpolarizing action of inhibitory neurotransmitters (1–5). Accordingly, null mice die perinatally (2), and loss of the splice variant KCC2b leads to generalized seizures (6). KCC2 is further involved in neuroprotection (7), stress response (8), and neuropathic pain (9). In contrast, truncation of KCC3 causes a severe peripheral neuropathy, often accompanied by agenesis of the corpus callosum (10, 11). Finally, targeted deletion of murine KCC4 results in renal tubular acidosis and deafness (12).

KCC proteins share considerable conservation of primary sequence; KCC1 and KCC3 exhibit 75% identity, and KCC2 and KCC4 share 72% of their amino acid residues (13). The sequence identity between KCC1 and KCC3 on one hand and KCC2 and KCC4 on the other hand is ~65% (13). All members are thought to possess a similar architecture. The current topology models predict 12 transmembrane domains (TMDs) with a large glycosylated loop between TMDs 5 and 6; both termini are cytoplasmic (14, 15). The transporters probably become functional by forming oligomers. Coexpression of a truncated transport-inactive KCC1 inhibited transport activity of other KCCs (16), and biochemical analysis demonstrated oligomeric forms of KCCs (17–20). A similar organization of the transporters is supported by identical functional consequences of mutations. Substitution of Tyr^{1087} to aspartate in KCC2 or its congener in KCC1 reduced transport activity (21). Furthermore, replacement of threonines by alanine at positions 991 and 1048 in KCC3 or their congeners in KCC2 increased transport activity (22).

Despite the overall structural similarity, heterologous expression analyses have revealed marked functional differences between KCCs, encompassing sensitivity to loop diuretics, ion affinities, and transport activity under isotonic conditions (13). These differences were observed not only between the two subfamilies but also within a given subfamily. Biochemical analyses of the closely related KCC2 and KCC4, for

* This work was supported, in whole or in part, by National Institutes of Health Grant DK57708 (to D. B. M.). This work was also supported by Deutsche Forschungsgemeinschaft Grant 428/2-3 (to H. G. N.).

[S] The on-line version of this article (available at http://www.jbc.org) contains supplemental Figs. 1–5.

[1] Present address: Institute for Experimental and Clinical Pharmacology and Toxicology, University of Saarland, Bldg. 46, 66421 Homburg, Germany.

[2] To whom correspondence should be addressed: Dept. of Neurogenetics, Carl von Ossietzky University of Oldenburg, D-26111 Oldenburg. Tel.: 49-441-798-3932; Fax: 49-441-798-3250; E-mail: hans.g.nothwang@uni-oldenburg.de.

[3] The abbreviations used are: KCC, K^+Cl^- cotransporter; TMD, transmembrane domain; LEL, large extracellular loop; ANOVA, analysis of variance; $KCC2_{wt}$, wild-type KCC2; NEM, *N*-ethylmaleimide.

TABLE 1
Description of complex KCC mutants

Clone abbreviation	Comment	KCC2 residues (GenBank™ NM_134363)	KCC4 residues (GenBank™ NM_011390)	Mutation
KCC2q	Quadruple mutated extracellular loop	1–1116		C287S,302L,C322S,C331L
$KCC2_{2\text{-}4\text{-}2}$	Extracellular loop of KCC4	1–276, 399–1116	298–418	
$KCC2_{2\text{-}4q\text{-}2}$	Quadruple mutated extracellular loop of KCC4	1–276, 399–1116	298–418	C308S,C323L,C343S,C352L
KCC4q	Quadruple mutated extracellular loop		1–1103	C308S,C323L,C343S,C352L
$KCC4_{4\text{-}2\text{-}4}$	extracellular loop of KCC2	277–402	1–297, 423–1103	
$KCC4_{4\text{-}2q\text{-}4}$	Quadruple mutated extracellular loop of KCC2	277–402	1–297, 423–1103	C287S,302L,C322S,C331L

instance, demonstrated several differences. Most strikingly, KCC2 is active under isotonic conditions (23), whereas KCC4 mediates significant cotransport only under hypoosmotic conditions (24). Furthermore, KCC2 has a high affinity to potassium and a low affinity to chloride (23), whereas KCC4 shows an equal affinity to both ions (24). Finally, the IC_{50} for the loop diuretic furosemide is considerably lower for KCC2 than for KCC4 (~50 *versus* ~900 μM) (13, 24, 25).

The underlying structural differences of these distinct properties are poorly understood. Mutational analyses have so far tackled the intracellular C terminus and the transmembrane domains, identifying a C-terminal domain that is required for the activity of KCC2 under isotonic conditions (26, 27). Here, we analyzed the sequence requirements of the large extracellular loop (LEL) between TMDs 5 and 6 in the closely related cotransporters KCC2 and KCC4 and addressed its role for binding to loop diuretics. Our results, obtained from 26 mutants, demonstrate an unexpected heterogeneity in the extracellular face of KCCs.

EXPERIMENTAL PROCEDURES

Plasmid Constructs—The open reading frames of rat KCC2b (GenBank™ accession number NM_134363) and mouse KCC4 (GenBank™ accession number NM_011390) were cloned into the pENTR/D-Topo vector (Invitrogen). Primers used were 5′-CACCATGCTCAACAACCTGACGG-3′ (forward) and 5′-TCAGGAGTAGATGGTG-3′ (reverse) for KCC2b and 5′-CACCATGCCCACGAACTTTACGGTG-3′ (forward) and 5′-TTAGGAGTAGATGGTGATGACT-3′ (reverse) for KCC4. Positive clones were verified by sequencing. Verified clones were transferred into a gateway pCDNA3.1 destination vector (Invitrogen).

Construction of Mutant and Chimeric cDNAs—Site-directed mutagenesis of KCC2b cDNA was performed according to the QuikChange mutagenesis system (Stratagene, Heidelberg, Germany). Oligonucleotides for the generation of the mutations were as follows (only forward primers are given): $KCC2_{C287S}$, 5′-TCGATCCACCCAATTTCCCGATTTCGCTCCTGGGGAA-3′; $KCC2_{C287L}$, 5′-CCACCCAATTTCCCGATTCTGCTCCTGGGGAACCGCAC-3′; $KCC2_{C302S}$, 5′-CCATGGCTTTGATGTCAGTGCCAAGCTGGCTTG-3′; $KCC2_{C302L}$, 5′-CTCGCCATGGCTTTGATGTCTTAGCCAAGCTGGC-3′; $KCC2_{C322S}$, 5′-GGCTCTGGGGCCTATTCTCGTCCTCCCGCCTCCTCAATG-3′; $KCC2_{C331L}$, 5′-CCTCCTCAATGCCACCTTAGATGAGTACTTCACCCG-3′. Mutant KCC4 was amplified from the *Xenopus* expression vector pGEMHE[4] and cloned into pCDNA3.1. To express KCC2b mutants in *Xenopus laevis* oocytes, the respective open reading frame was amplified from the mammalian expression vector by PCR and cloned into pGEMHE.

For construction of chimeric clones that contained the LEL of the paralogous transporter, we took advantage of the strong conservation of TMDs 5 and 6 in KCC2 and KCC4. The respective wild-type or mutated LEL was amplified using the degenerate primers KCCel-for (5′-ATCCTGGCCATCTAYGCWGGKGTCATCAAG-3′) and KCCel-rev (5′-TAGATGCCAACWAGCAKGGTGAAGTAGG-3′). Purified PCR products were used as megaprimers to construct chimeric clones with the paralogous KCC clone as template (28). These resulted in chimeric clones with the junctions located in TMDs 5 and 6 (Table 1). All generated clones used in this study were confirmed by sequencing.

Determination of K^+-Cl^- Cotransport—Transport activity was determined by measuring Cl^--dependent uptake of $^{86}Rb^+$ (PerkinElmer Life Sciences) in HEK-293 cells or *X. laevis* oocytes. HEK-293 cells were cultured in Dulbecco's modified Eagle's medium (Invitrogen) and transfected using TurboFect (Fermentas, St. Leon-Roth, Germany). Cells were harvested 48 h after transfection, transferred into poly-L-lysine-coated wells of a 6-well culture dish, incubated for 3 h. After removal of the medium, cells were incubated in 1 ml of preincubation buffer (100 mM *N*-methyl-D-glucamine chloride, 5 mM KCl, 2 mM $CaCl_2$, 0.8 mM $MgSO_4$, 5 mM glucose, 5 mM HEPES, pH 7.4, 0.1 mM oubain) for 15 min at room temperature. A 10-min uptake period followed in preincubation buffer supplemented with 1 μCi/ml $^{86}Rb^+$ at room temperature. At the end of the uptake period, cells were washed three times in 1 ml of ice-cold preincubation buffer to remove extracellular tracer. Cells were lysed in 500 μl of 0.25 M NaOH for 1 h and then neutralized with 250 μl of pure acetic acid. $^{86}Rb^+$ uptake was assayed by Cerenkov radiation, and the protein amount was determined by BCA (Thermo Fisher Scientific, Bonn, Germany). To determine the concentration-response profile, increasing concentrations of furosemide (2–2,000 μM) were applied to the preincubation and uptake buffer. In addition, expression of the respective construct was determined for each flux measurement by immunoblot analysis. Three biological and three technical replicas were performed for each experiment. Data are given as means ± S.D. Significant differences between the groups were analyzed by Student's *t* test or with a one-way ANOVA.

In some experiments, non-radioactive flux measurements based on thallium (Tl^+)-mediated fluozin-2 fluorescence were performed (29). 24 h after transfection, HEK-293 cells were plated in poly-L-lysine-coated wells of a 96-well culture dish, black-walled with clear bottom (Greiner Bio-One) at a concentration of 100,000 cells/well. The next day, the medium was

[4] A. Mercado, E. Babilonia, D. B. Mount, manuscript in preparation.

replaced by 80 μl of preincubation buffer (100 mM *N*-methyl-D-glucamine chloride, 5 mM KCl, 2 mM $CaCl_2$, 0.8 mM $MgSO_4$, 5 mM glucose, 5 mM HEPES, pH 7.4) with or without 2 μM flouzin-2 dye (Invitrogen) plus 0.2% (w/v) Pluronic F-127 (Invitrogen). Cells were incubated at room temperature for 48 min. Afterward, the cells were washed 3 times with 80 μl of preincubation buffer and incubated for 15 min with 80 μl of preincubation buffer plus 0.1 mM ouabain. Then the cell plate was inserted into a fluorometer (Fluoroskan Accent, Thermo Scientific, Bremen, Germany), and the wells were injected with 40 μl of 5× thallium stimulation buffer (12 mM thallium sulfate, 100 mM NMDG, 5 mM Hepes, 2 mM calcium sulfate, 0.8 mM magnesium sulfate, 5 mM glucose, pH 7.4). The fluorescence was measured in a kinetic-dependent manner (excitation, 485 nm; emission, 538 nm; 1 frame in 5 s in a 200-s time span). The activity was calculated with the initial values of the slope of Tl^+-stimulated fluorescence increase by using linear regression.

Transport activity in *X. laevis* oocytes was assessed by measuring Cl^--dependent $^{86}Rb^+$ uptake under hypotonic conditions. Oocytes were surgically collected from animals anesthetized by 0.17% tricaine immersion. After extraction, oocytes were incubated for 1 h with vigorous shaking in a Ca^{2+}-free ND96 medium (96 mM NaCl, 2 mM KCl, 1 mM MgCl, and 5 mM HEPES/Tris, pH 7.4, plus 2 mg/ml collagenase A) and then washed four times in regular ND96 medium, defolliculated, and incubated overnight in ND96 at 16 °C. Mature oocytes were injected with 50 nl of 100 mM Tris, pH 7.4, or with 100 mM Tris, pH 7.4, containing 25 ng of KCC cRNA transcribed *in vitro*. Oocytes were incubated for 2–3 days prior to transport assays in ND96 at 16 °C supplemented with 2.5 mM sodium pyruvate, 5 mg/100 ml gentamicin, and 20 μM bumetanide. On the day of the influx measurements, oocytes were incubated for 30 min in a Cl^--free medium (50 mM *N*-methyl-D-glucamine gluconate, 10 mM potassium gluconate, 4.6 mM calcium gluconate, 1 mM magnesium gluconate, 5 mM HEPES/Tris, pH 7.4) containing ouabain (1 mM), followed by a 60-min uptake period in a Na^+-free medium (40 mM *N*-methyl-D-glucamine-Cl, 10 mM KCl, 1.8 mM $CaCl_2$, 1 mM $MgCl_2$, 5 mM HEPES/Tris, pH 7.4) supplemented with ouabain and 2.5 μCi/ml $^{86}Rb^+$. All uptake assays were performed at 32 °C. At the end of the uptake period, oocytes were washed three times in ice-cold uptake solution without isotope to remove extracellular fluid tracer. Oocytes were dissolved in 10% SDS, and tracer activity was determined for each oocyte by β-scintillation counting.

Cell Surface Biotinylation—Cell surface expression levels were assessed by surface biotinylation. For this purpose, 90–95% confluent 10-cm culture dishes of transfected HEK-293 cells were treated with the membrane-impermeant sulfosuccinimidyl 2-(biotinamido)-ethyl-1,3-dithiopropionate (Thermo Fisher Scientific), according to the provided protocol. After several washes and cell lysis, biotinylated proteins were recovered by a NeutrAvidin-agarose column. After three rounds of washes, biotinylated proteins were eluted in sample buffer. Aliquots of the cell homogenate and of the eluate were collected and analyzed by immunoblot analysis.

To quantify the amount of KCCs expressed at the cell surface, dilution series of each sample were loaded onto a 10% SDS-polyacrylamide gel system. After separation and electrotransfer onto polyvinylidene difluoride membranes, the membranes were incubated with anti-cKCC2 (dilution 1:1,000) (17) or anti-KCC4 (dilution 1:1,000) (30). After incubation for 2 h at room temperature, membranes were washed four times with TBS-T (20 mM Tris, 150 mM NaCl, 1% Tween, pH 7.5), and the secondary antibody donkey anti-rabbit IgG-horseradish peroxidase (Santa Cruz Biotechnology, Heidelberg, Germany) was applied for 1 h. After washing, bound antibodies were detected using an enhanced chemiluminescence assay (GE Healthcare) and a LAS-3000 documentation system (Fujifilm, Düsseldorf, Germany). Quantification of the bands was performed using the MultiGauge software version 3.1 (Fujifilm). The cell lysate corresponds to the total protein amount and was set to 100%. Only data with recovery values of 100 ± 20% were included in our analysis. Four biological and three technical replicas were performed for each construct. Data are given as mean ± S.D. Significant differences between the groups were analyzed by a Student's *t* test.

Immunocytochemistry—For immunocytochemistry, transfected cells were seeded on 0.1 mg/ml poly-L-lysine-coated coverslips. After 36 h, cells were fixed with 4% paraformaldehyde in 0.2 M phosphate buffer for 10 min. After fixation, cells were washed three times with phosphate-buffered saline and incubated with blocking solution (0.3% Triton X-100, 3% bovine serum albumin, 10% goat serum in phosphate-buffered saline) for 30 min. All steps were performed at room temperature. The cells were incubated with primary antibody solution (anti-cKCC2, 1:500) (17) in blocking solution for 30 min and washed three times with phosphate-buffered saline for 5 min. Thereafter, the secondary antibody was added, which was conjugated to a fluorescent probe (1:1,000; Alexa Fluor 488 goat anti-rabbit (Invitrogen)). After washing, cells were mounted onto glass slides with Vectorshield Hard Set (Vector Laboratories, Burlingame, CA). Photomicrographs were taken using an Axioskop microscope with a ×100 objective (Zeiss, Oberkochen, Germany).

RESULTS

Evolutionary Conservation of Cysteines in the LEL between TMDs 5 and 6—To initiate structure-function studies of the LEL of rat KCC2, we focused on its highly conserved cysteines. According to the hydrophobicity-based topology model of KCC2 (14), which is supported by biochemical data of the related family member NKCC1 (31), the LEL of KCC2 encompasses the amino acids 275–399 of KCC2b (32). The KCC2a and KCC2b isoforms differ in the use of different N-terminal first coding exons; this study utilizes rat KCC2b, hereafter referred to as KCC2. The LEL contains four cysteine residues that are conserved in all four mammalian KCCs isoforms (positions 287, 302, 322, and 331 of rnKCC2; Fig. 1). Moreover, alignment with KCC sequences from *Danio rerio*, *Drosophila melanogaster*, and *Caenorhabditis elegans* demonstrated evolutionary conservation of three of them (Cys^{287}, Cys^{322}, and Cys^{331}) across all three species. Cys^{302} was only absent in *C. elegans* (Fig. 1). Notably, the four cysteines belonged to the most highly conserved amino acids within the 124-amino acid-long LEL. Only four other amino acid residues (Leu^{294}, Gly^{348},

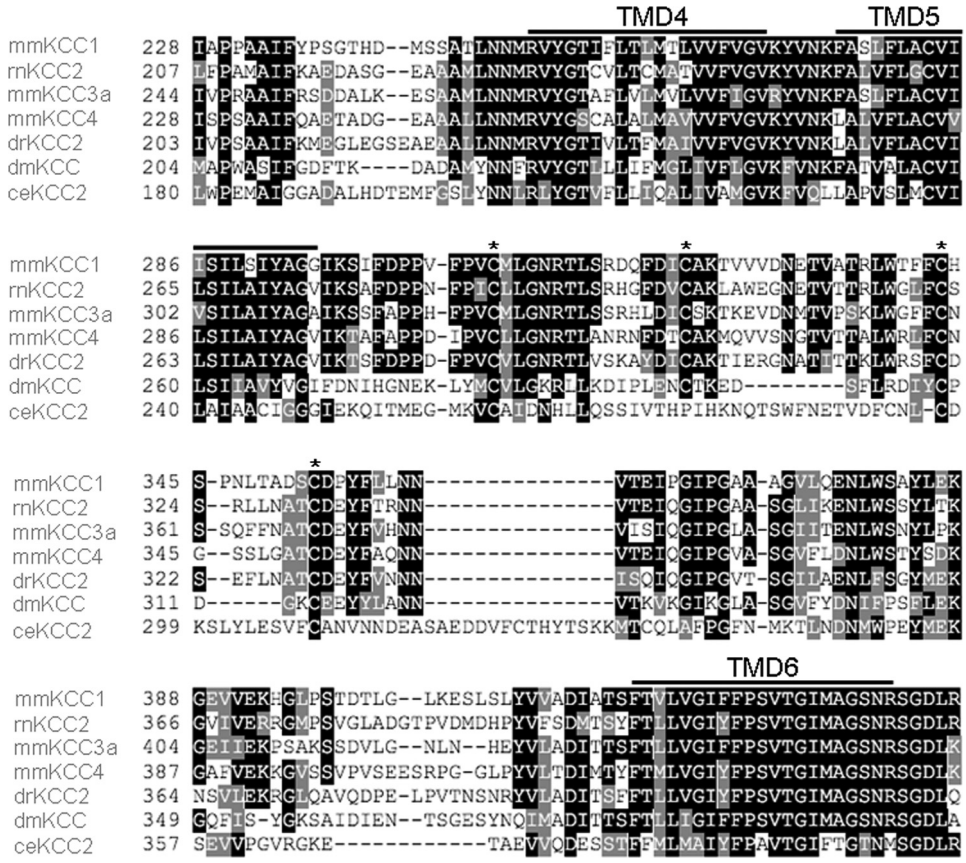

FIGURE 1. **Cysteines of the large extracellular loop are highly conserved.** Partial alignment of KCCs reveals high conservation of the four cysteines (marked with an *asterisk*) in the LEL between TMDs 5 and 6. The prediction of the TMDs is according to the hydropathy model of KCC2 (14). *mm*, *Mus musculus*; *rn*, *Rattus norvegicus*; *dr*, *D. rerio*; *dm*, *D. melanogaster*; *ce*, *C. elegans*.

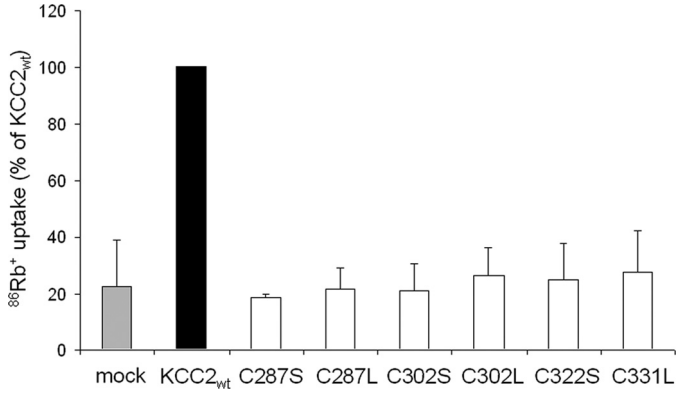

FIGURE 2. **Single cysteine mutations in the LEL abolish transport activity of KCC2.** HEK-293 cells were assayed for $^{86}Rb^+$ uptake 48 h after transfection with the constructs indicated *below* the *columns*. An empty vector was used for mock transfection. KCC2 wild type ($KCC2_{wt}$)-transfected cells displayed a 5 times higher activity compared with mock-transfected cells. All single cysteine mutants in the extracellular loop of KCC2 were transport-inactive because their transport activity showed no significant difference from the empty vector. The plot depicts the mean of three experiments ± S.D. (*error bars*). One-way ANOVA of all determinants demonstrated a significant multivariate effect ($F = 198.67$; $p < 0.001$). ANOVA without $KCC2_{wt}$ revealed no significant difference between mutants and mock-transfected cells ($F = 0.3$; $p = 0.94$).

Lys[365], and Asp[395]) were conserved in all species that we analyzed (Fig. 1). The high conservation of cysteines across orthologs and paralogs implies an important role for these cysteines in KCC2 function.

Mutagenesis of Individual Cysteine Residues Abolishes Transport Activity of KCC2—To analyze the role of the four cysteines for KCC2 transport activity, we first replaced them individually by serine or leucine. This resulted in the four mutants $KCC2_{C287S}$, $KCC2_{C302L}$, $KCC2_{C322S}$, and $KCC2_{C331L}$. We refrained from alanine as the general replacement residue because serine and leucine substitutions were among the best tolerated in the murine KCC4 paralog.[4] To evaluate the effect of the mutations, the constructs were transiently expressed in HEK-293 cells. First, we assessed their expression by immunocytochemistry. KCC2 immunoreactivity was detected for all four mutants both at the plasma membrane and in the perinuclear region (supplemental Fig. 1). Only the nucleus was spared. The labeling pattern of the KCC2 mutants was similar to that obtained in wild-type KCC2 ($KCC2_{wt}$; compare supplemental Fig. 1 and Fig. 5*B*). We therefore conclude that the mutations did not affect protein expression and localization.

We next determined transport activity by $^{86}Rb^+$ flux measurements. To eliminate any $^{86}Rb^+$ flux mediated through endogenous NKCC1, the experiments were performed in Na^+-free solution with *N*-methyl-D-glucamine being the replacement cation (33, 34). HEK-293 cells transiently expressing $KCC2_{wt}$ displayed a significantly higher $^{86}Rb^+$ uptake (100%) than mock-transfected control cells (22.3 ± 16.5%; Fig. 2). Interestingly, mutating each of the four cysteines abolished transport activity (Fig. 2). To analyze whether other substitutions do not disrupt function, we generated the mutants $KCC2_{C287L}$ and $KCC2_{C302S}$ in addition to $KCC2_{C287S}$ and $KCC2_{C302L}$. Immunocytochemistry showed that both novel mutants were expressed with no visible difference to $KCC2_{wt}$ (compare supplemental Fig. 1 and Fig. 5*B*). $^{86}Rb^+$ flux measurements revealed that these replacements resulted in non-functional KCC2, like the previous ones (Fig. 2). Taken together, these results demonstrate that individual cysteine residues in the LEL are not essential for KCC2 expression, but they are required for transport activity.

KCC2 Compound Cysteine Mutants Are Non-functional—The four cysteine residues in the LEL are potentially involved in the formation of intra- or intermolecular disulfide bonds. Hence, the elimination of single cysteines can result in non-native, abnormal disulfide bonds, thereby modifying the structure and rendering KCC2 non-functional, as previously shown for the ATP binding cassette transporter ABCG2 (35). We therefore tested whether transport activity could be restored by

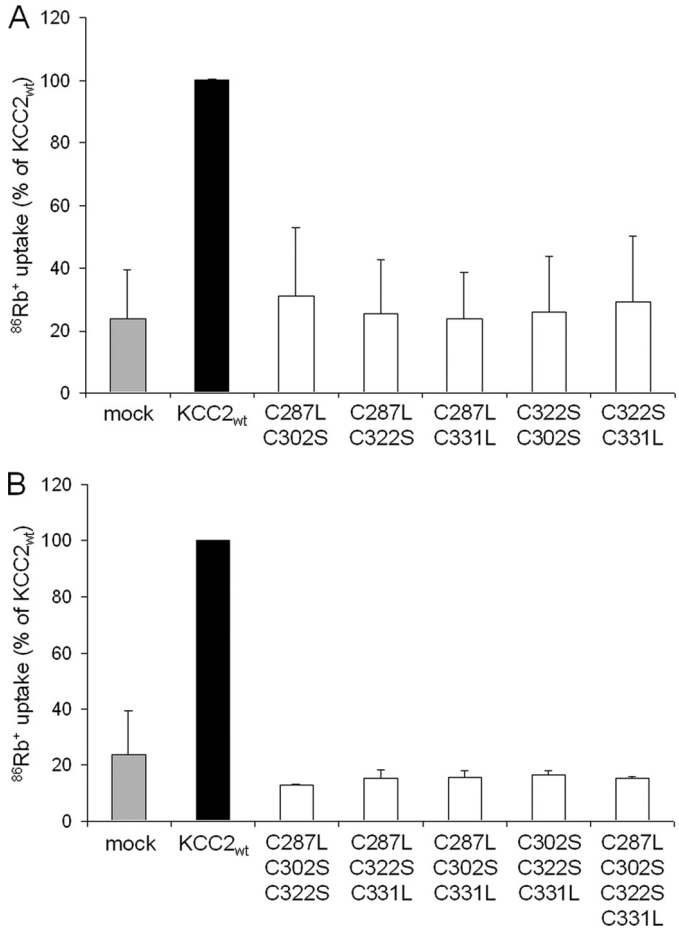

FIGURE 3. **Double, triple, and quadruple cysteine KCC2 mutants are transport-inactive.** The $^{86}Rb^+$ uptake of $KCC2_{wt}$ and compound mutants were measured in transfected HEK-293 cells. All double cysteine (*A*) and triple and quadruple cysteine (*B*) KCC2 mutants were transport-inactive because their transport activity showed no significant difference from the empty vector. Plots depict mean of three experiments ± S.D. (*error bars*). One-way ANOVA of all determinants demonstrated a significant multivariate effect for the double mutants ($F = 31.1$; $p < 0.001$) and for the triple and quadruple mutants ($F = 3316.99$; $p < 0.001$). ANOVA without $KCC2_{wt}$ revealed no significant difference between the double mutants ($F = 0.16$; $p = 0.98$) or the triple and quadruple mutants ($F = 1.64$; $p = 0.17$) compared with mock-transfected cells.

elimination of additional cysteines. To do so, we generated a total of 10 compound mutants, consisting of five double mutants, four triple mutants, and one quadruple mutant. Double mutants comprised $KCC2_{C287L,C302S}$, $KCC2_{C287L,C322S}$, $KCC2_{C287L,C331L}$, $KCC2_{C302S,C322S}$, and $KCC2_{C302S,C331L}$; triple mutants comprised $KCC2_{C287L,302S,C322S}$, $KCC2_{C287L,302S,C331L}$, $KCC2_{C287L,322S,C331L}$, and $KCC2_{C302S,C322S,C331L}$; and the quadruple mutant consisted of $KCC2_{C287L,C302S,C322S,C331L}$. Again, we first analyzed the expression and localization of these 10 compound mutants in HEK-293 cells by immunocytochemistry. All mutants were expressed, and their labeling pattern was indistinguishable from $KCC2_{wt}$ (compare supplemental Fig. 2 and Fig. 5*B*). Determination of $^{86}Rb^+$ uptake revealed that all compound mutants were non-functional (Fig. 3). The failure of the compound mutants to rescue transport activity suggests that loss of transport activity in single cysteine mutants is not caused by non-native disulfide bonds within the LEL.

LEL Cysteine Mutations Differentially Affect Transport Activity of KCC2 and KCC4—The results obtained so far for KCC2 are in contrast to a cysteine analysis performed in the murine KCC4.[4] In this paralog, mutations of any of the cysteines at the corresponding positions 308, 323, 343, and 352 or of all four cysteines did not abolish transport activity upon expression in *X. laevis* oocytes. One explanation for this discrepancy is the use of different expression systems, namely amphibian *X. laevis* oocytes for KCC4 and mammalian HEK-293 cells for KCC2. To address this issue, we first cloned our single cysteine mutants ($KCC2_{C287S}$, $KCC2_{302L}$, $KCC2_{C322S}$, and $KCC2_{C331L}$) into a *Xenopus* expression vector and determined their transport activity in *X. laevis* oocytes. In contrast to their KCC4 paralogs,[4] none of the four KCC2 mutants mediated $^{86}Rb^+$ uptake (supplemental Fig. 3). Additionally, we expressed the four KCC4 single cysteine mutants in HEK-293 cells (supplemental Fig. 4). They showed significant transport activity above background (supplemental Fig. 5).

To further assess whether different expression systems may cause different results, we cloned KCC4 and its quadruple mutant $KCC4_q$ in a mammalian expression vector and generated a second quadruple $KCC2_{C287S,C302L,C322S,C331L}$ mutant, $KCC2_q$, which contains cysteine replacements identical to those in the $KCC4_q$ mutant. We then performed flux measurements in HEK-293 cells. $KCC2_q$ showed a low, albeit detectable, transport activity (Fig. 4*A*), which was 23 ± 5.2% of $KCC2_{wt}$ ($p < 0.001$) after background subtraction. The immunocytochemical analysis showed similar expression patterns of $KCC2_{wt}$ and $KCC2_q$ (Fig. 5*B*). KCC4-expressing HEK-293 cells displayed a significantly higher $^{86}Rb^+$ uptake (100%) than mock-transfected control cells (12.87 ± 5.06%, $p < 0.001$; Fig. 4*B*). For the quadruple mutant $KCC4_q$, we observed a transport activity similar to $KCC4_{wt}$ (Fig. 4*B*). The results indicate that the different expression systems cannot account for the observed differences between KCC2 and KCC4.

A characteristic feature of KCCs is their activation by the cysteine-reactive compound *N*-ethylmaleimide (NEM) (36). We therefore asked the question whether NEM can rescue transport activity in the mutant KCC2. $KCC2_{wt}$ and $KCC4_{wt}$ as well as the quadruple mutant $KCC4_q$ were activated 2-fold after treatment with 1 mM NEM for 15 min (Fig. 4, *A* and *B*). In contrast, the transport-inactive quadruple mutant $KCC2_q$ could not be activated by NEM (Fig. 4*A*). To sum up, identical replacements of cysteine residues in the LEL differentially affected the transport activity of the closely related KCC family members KCC2 and KCC4, independent of the expression system employed. The striking difference between $KCC2_q$ and $KCC4_q$ indicates differential requirement of cysteines in the LEL for KCC2 and KCC4 transport activity.

Chimeras Confirm Differences in the LEL between KCC2 and KCC4—The amino acid sequences in the LEL of KCC2 and KCC4 are rather divergent, with only 55.2% shared identities compared with 72% identify over the entire length of the two proteins. This indicates that the different requirement of the four cysteines regarding transport activity is caused by a distinct structural organization of their LELs. To test this hypothesis, we created KCC2 and KCC4 chimeras in which we swapped the wild-type or quadruple mutated LEL between the

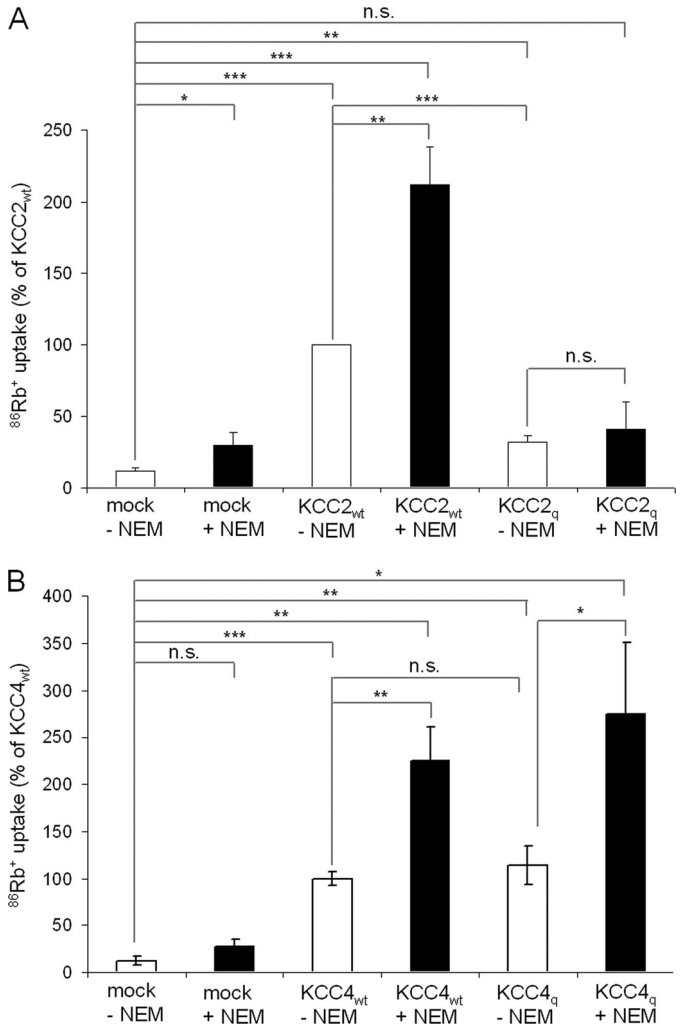

FIGURE 4. **Cysteine mutations in the LEL differentially affect transport activity of KCC2 and KCC4.** HEK-293 cells were assayed for $^{86}Rb^+$ uptake 48 h after transfection with the constructs indicated *below* the *columns*. An empty vector was used for mock transfection. *A*, $^{86}Rb^+$ uptake of the quadruple cysteine mutant $KCC2_q$ (C287S,C302L,C322S,C331L) resulted in a decrease of the transport activity compared with $KCC2_{wt}$ ($p < 0.001$). Treatment with 1 mM NEM did not increase the transport activity of the quadruple mutant in contrast to its effect on $KCC2_{wt}$. *B*, KCC4-transfected cells revealed increased transport activity in relation to mock-transfected cells. $^{86}Rb^+$ uptake of $KCC4_{wt}$ and the quadruple mutant $KCC4_q$ (C308S,C323L,C343S,C352L) is similar. The plot depicts the mean of three experiments ± S.D. (*error bars*). ***, $p < 0.001$; *n.s.*, not significant.

two paralogs (Fig. 5*A*). This resulted in the chimeras $KCC2_{2\text{-}4\text{-}2}$ and $KCC4_{4\text{-}2\text{-}4}$ (swapping of wild type), as well as $KCC2_{2\text{-}4q\text{-}2}$ and $KCC4_{4\text{-}2q\text{-}4}$ (swapping of mutant LEL). Upon expression of the chimeras in HEK-293 cells, immunocytochemical or immunoblot analysis confirmed the expression of the chimeras (Fig. 5, *B* and *C*).

Swapping the wild-type LEL differentially affected the transport activity of KCC2 and KCC4. The transport activity of $KCC2_{2\text{-}4\text{-}2}$ (99.88 ± 7.76%), after background subtraction, was equal to that of $KCC2_{wt}$ (100%, $p = 0.98$; Fig. 6*A*). In contrast, $KCC4_{4\text{-}2\text{-}4}$ was transport-inactive (Fig. 6*B*). Functional analysis of the chimeras containing the quadruple mutated LEL revealed that the activity of $KCC4_{4\text{-}2q\text{-}4}$ was completely abolished and strongly reduced for $KCC2_{2\text{-}4q\text{-}2}$ (13.97 ± 6.15%; Fig. 6). Thus, the mutated KCC4 LEL rendered KCC2 transport-inactive, despite the fact that the mutation did not affect transport activity in KCC4. These data indicate that cysteines in the LEL play an important role for the overall conformation of KCC2. This contrasts with KCC4 function, which apparently does not require LEL cysteines.

Sensitivity to Furosemide Depends on the LEL—KCC2 and KCC4 markedly differ in their sensitivity to loop diuretics; KCC2 displays the lowest (~50 μM) and KCC displays the highest IC_{50} value (~900 μM) among the four KCC family members (13, 24, 25). To investigate whether the observed structural differences in the LEL contribute to this difference, we performed dose-response curves in HEK-293 cells for the inhibition by furosemide using KCC2, KCC4, and $KCC2_{2\text{-}4\text{-}2}$, the only transport-active chimera (Fig. 7). We obtained IC_{50} values of 184.4 μM ($R^2 = 0.96695$) and 548.8 μM ($R^2 = 0.98556$) for KCC2 and KCC4, respectively, confirming the higher furosemide affinity of KCC2. The IC_{50} of $KCC2_{2\text{-}4\text{-}2}$ was 396.5 μM ($R^2 = 0.97714$; Fig. 7). This value thus differed from that of KCC2 and was closer to that of KCC4. The data suggest that the LEL is involved in binding of the loop diuretics and that the structural differences between the KCC isoforms therein shape the sensitivity to loop diuretics.

Transport-inactive KCCs Are Expressed at the Cell Surface—The loss of transport activity observed in the mutants and chimeras may arise from reduced expression, misrouting, or conformational changes. Our previous immunocytochemical and immunoblot analyses indicated that cysteine mutations in KCC2 do not impair its expression. To analyze trafficking to the plasma membrane, we performed cell surface labeling of selected KCC constructs. The proteins analyzed included the transport-active isoforms $KCC2_{wt}$ and $KCC4_{wt}$ as well as the transport-inactive or impaired $KCC2_q$, $KCC2_{2\text{-}4q\text{-}2}$, $KCC4_{4\text{-}2\text{-}4}$, and $KCC4_{4\text{-}2q\text{-}4}$. The cell surface expression of $KCC2_q$ (8.2 ± 2.1%) did not significantly differ from $KCC2_{wt}$ (13.2 ± 4.6%, $p = 0.1$), whereas $KCC2_{2\text{-}4q\text{-}2}$ (6.3 ± 2.1%, $p = 0.02$) displayed a 2-fold reduction in cell surface expression compared with $KCC2_{wt}$ (Fig. 8*A*). No difference was observed for $KCC4_{wt}$, $KCC4_{4\text{-}2\text{-}4}$, and $KCC4_{4\text{-}2q\text{-}4}$ (Fig. 8*B*). Hence, most transport-inactive KCC variants are routed normally to the plasma membrane. The only exception was $KCC2_{2\text{-}4q\text{-}2}$, whose surface expression amounted to ~50% compared with $KCC2_{wt}$. This reduction, however, does not explain the >85% loss in transport activity. These findings suggest that the loop substitutions across the transporters mainly affect their ion translocation properties.

DISCUSSION

Via site-directed mutagenesis and generation of chimeras, we have investigated the sequence requirements of the LEL in KCC2 and KCC4 for protein expression, function, and drug binding. The main finding of our study is that transport function of KCC2 and KCC4 depends on different sequence requirements of the LEL. In contrast to KCC4, elimination of all four evolutionary conserved cysteines in the LEL reduced KCC2 transport activity by more than 75%. In addition, the LEL of KCC2 requires the parental backbone, whereas the LEL of KCC4 also functions together with the homologous backbone of KCC2 ($KCC2_{2\text{-}4\text{-}2}$). Another interesting observation was that

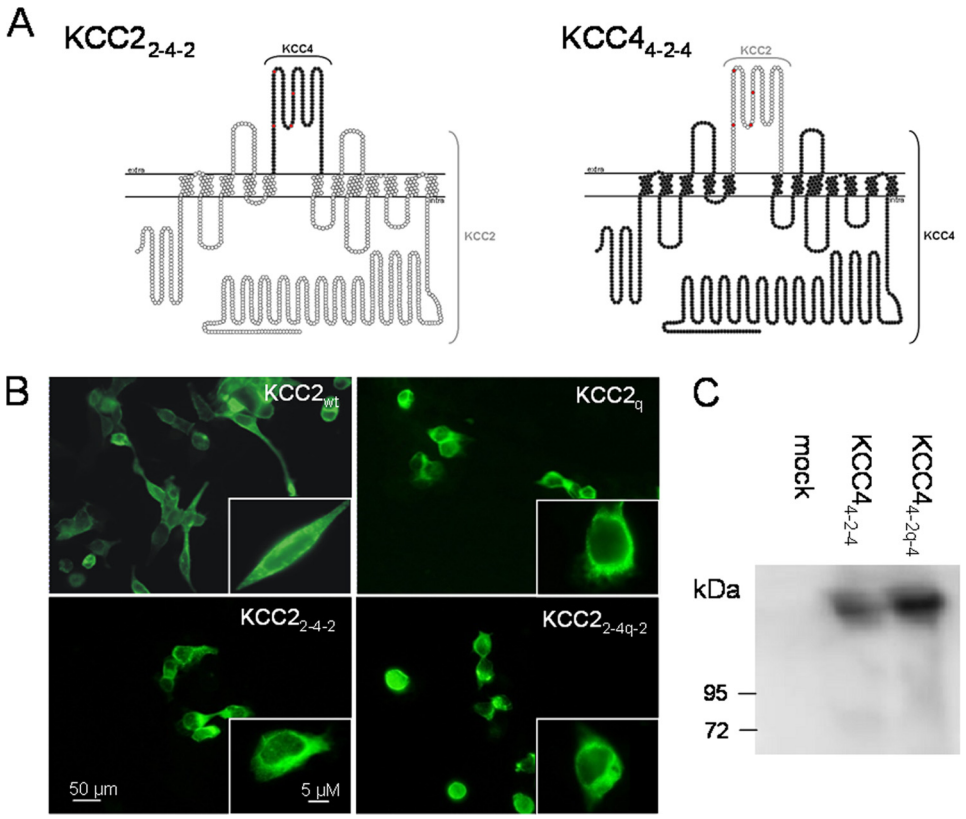

FIGURE 5. **Chimera of KCC2 and KCC4 are expressed in HEK-293 cells.** *A*, topology model of the chimeras KCC2$_{2-4-2}$ and KCC4$_{4-2-4}$. *White circles* and *black circles* represent amino acid residues of KCC2 and KCC4, respectively. The extracellular cysteines are marked in *red*. *B*, immuncytochemical labeling of KCC2$_{wt}$, the quadruple mutant KCC2$_{q}$, the chimera KCC2$_{2-4-2}$, and the quadruple cysteine mutant chimera KCC2$_{2-4q-2}$ upon transient transfection in HEK-293 cells. In the wild type and the mutants, KCC2 immunoreactivity was detected at the plasma membrane and the perinuclear region. *C*, immunoblot analysis of the chimera KCC2$_{4-2-4}$ and the quadruple cysteine mutant chimera KCC4$_{4-2q-4}$. Both chimeras are expressed in HEK-293 cells.

the LEL plays a role in the sensitivity of KCCs to loop diuretics. This was evidenced by the different IC_{50} values obtained for KCC2$_{wt}$ and its chimera KCC2$_{2-4-2}$, which differed only in the LEL.

Our analysis of the four evolutionary conserved cysteines in the LEL of KCC2 revealed their crucial requirement for transport activity. Each of the six generated single cysteine mutants was non-functional (Fig. 2). The importance of the extracellular cysteines for KCC2 transport activity was corroborated by the observation that the wild-type LEL of KCC4 but not the mutated one could replace the LEL of KCC2. This requirement of cysteines is in line with the related Na^+-K^+-Cl^- cotransporter NKCC1, which also requires any of the five cysteines present in the LEL between TMDs 7 and 8 to be transport-active (37). In contrast, KCC4 activity was only impaired by single cysteine mutants, and most importantly, the quadruple mutant of KCC4 is still fully active (Fig. 4*B*). The impaired transport activity of the single KCC4 mutants might be due to abnormal cysteine bonds.

We first considered the different expression systems as a possible explanation for this discrepancy (KCC2 mutants analyzed in HEK-293 cells (initial part of this study), KCC4 mutants analyzed in *X. laevis* oocytes).[4] However, after having performed subsequent reciprocal experiments (*i.e.* having analyzed KCC2 mutants in *Xenopus* oocytes and KCC4 mutants in HEK-293 cells), we can rule out this possibility (Fig. 4 and supplemental Fig. 3). Only for KCC4 single mutants did we observe an increased impairment of transport activity in HEK-293 cells compared with *X. laevis* oocytes (supplemental Fig. 5).[4] Thus, we propose a robust difference in requirements of cysteines in the LEL between KCC2 and KCC4. Our results also demonstrate that data arising from mutation analyses cannot easily be transferred to related KCC isoforms, even if their amino acids are highly conserved. It will be interesting to analyze the functional roles of the cysteines in the LEL of KCC1 and KCC3 as well, in order to find out whether they resemble KCC2, KCC4, neither, or both. Different effects after mutating conserved amino acids have also been reported for other transporters, such as the closely related ileal and hepatic sodium-dependent bile acid transporters Isbt and Ntcp (38) or the two chloride channels CLC-Kb and CLC-Ka (39). The underlying structural differences, however, have not been elucidated so far.

The precise role of the analyzed cysteines for KCC2 transport activity is still unknown. Our data point to subtle but important conformational changes. First, immunocytochemical and immunoblot analyses of all the 18 transport-inactive mutants analyzed in this study yielded expression levels comparable with that of KCC2$_{wt}$ (supplemental Figs. 1 and 2) (data not shown). The mutants thus appear to pass the quality control in the endoplasmatic reticulum. This suggests that they are not grossly misfolded, because this would probably result in premature degradation (40). Second, our biotinylation experiments demonstrated that elimination of all four cysteine residues in KCC2$_{q}$ still resulted in surface expression similar to KCC2$_{wt}$ (Fig. 8). This is in agreement with the immunocytochemical data on the mutants, which revealed for most of the mutants no apparent decrease in plasma membrane staining. These data indicate that the cysteines are dispensable for correct trafficking and membrane insertion. Even in the quadruple mutant KCC2$_{2-4q-2}$, surface expression was reduced by merely 50% (Fig. 8), which contrasts with the almost complete (>85%) loss transport activity (Fig. 6). Thus, reduced surface expression may contribute in some of our constructs to the observed drop in transport activity, but it is definitely not the major cause.

It is unclear whether the cysteine replacements effect oligomerization of the KCC2 transporter. We have recently presented evidence that KCC2 oligomers are connected by disulfide bridges (17), whereas a recent study has observed

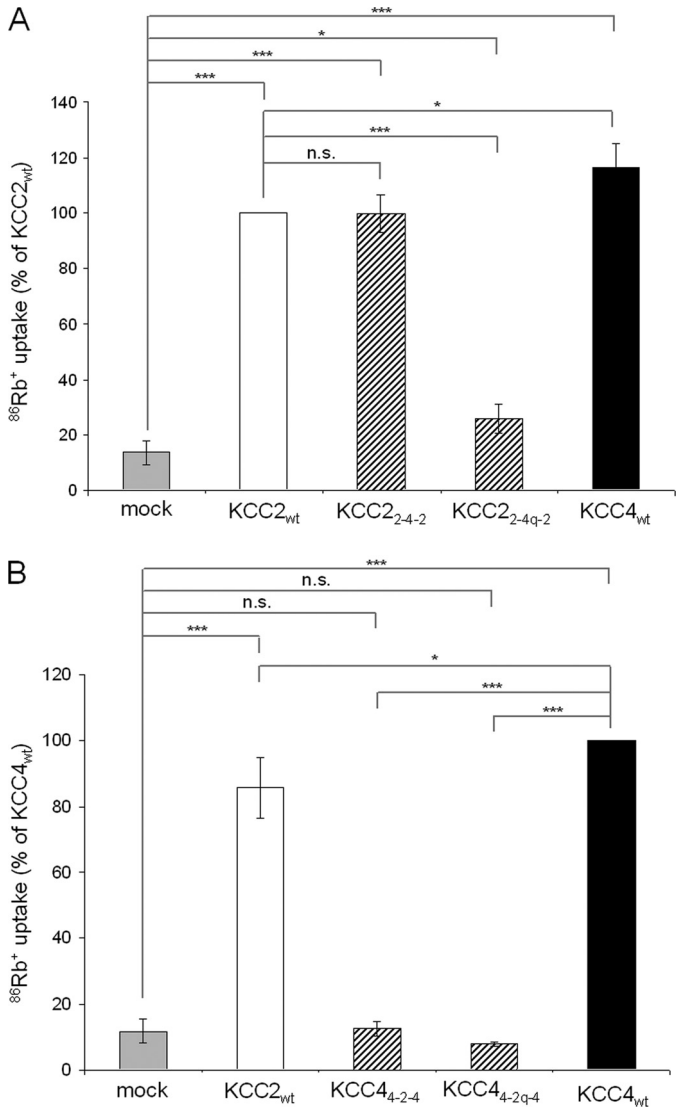

FIGURE 6. **The large extracellular loop of KCC2 but not of KCC4 requires the parental backbone.** HEK-293 cells were assayed for $^{86}Rb^+$ uptake 48 h after transfection with the constructs indicated *below* the *columns*. An empty vector was used for mock transfection. *A*, $KCC2_{wt}$ (*white bars*), $KCC4_{wt}$ (*black bars*), and the chimera $KCC2_{2-4-2}$ (*striped bars*) showed transport activity. The transport activity of $KCC2_{wt}$ and the chimera $KCC2_{2-4-2}$ is comparable. $KCC2_{2-4q-2}$ displayed strongly reduced transport activity compared with $KCC2_{wt}$ ($p < 0.001$). *B*, $KCC4_{4-2q-4}$ and $KCC4_{4-2-4}$ are transport-inactive. The plot depicts mean of three experiments ± S.D. ***, $p < 0.001$; *, $p < 0.05$; *n.s.*, not significant.

sensitivity of KCC2 oligomers to SDS (18). We could not investigate the oligomeric status of the KCC2 mutants because we noticed strong aggregation of the proteins after heterologous expression in HEK-293 cells,[5] which is consistent with the findings of Uvarov *et al.* (18). Therefore, future studies have to address the precise role of the cysteine residues, such as their involvement in intra- and intermolecular disulfide bonds.

The observed difference of the LEL between KCC2 and KCC4, together with the lower identity of the LEL (55.2%) compared with the total protein identity (72%), prompted us to investigate whether this region is involved in furosemide binding. The IC_{50} value of the transport-active chimera $KCC2_{2-4-2}$

[5] A. M. Hartmann and H. G. Nothwang, unpublished data.

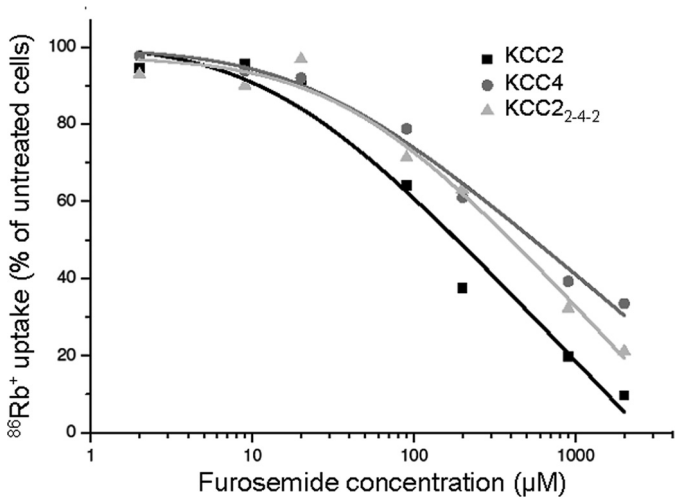

FIGURE 7. **Concentration-response profile for inhibition of KCC2, KCC4, and $KCC2_{2-4-2}$ by furosemide.** Transfected HEK-293 cells with KCC2, KCC4, and $KCC2_{2-4-2}$ were exposed to increased furosemide concentration from 2 to 2000 μM in the preincubation and uptake buffer. The activity of untreated cells of the respective KCC was normalized to 100%. IC_{50} values were determined by using logarithmic regression analysis. The plot depicts the mean of four experiments ± S.D. ***, $p < 0.001$.

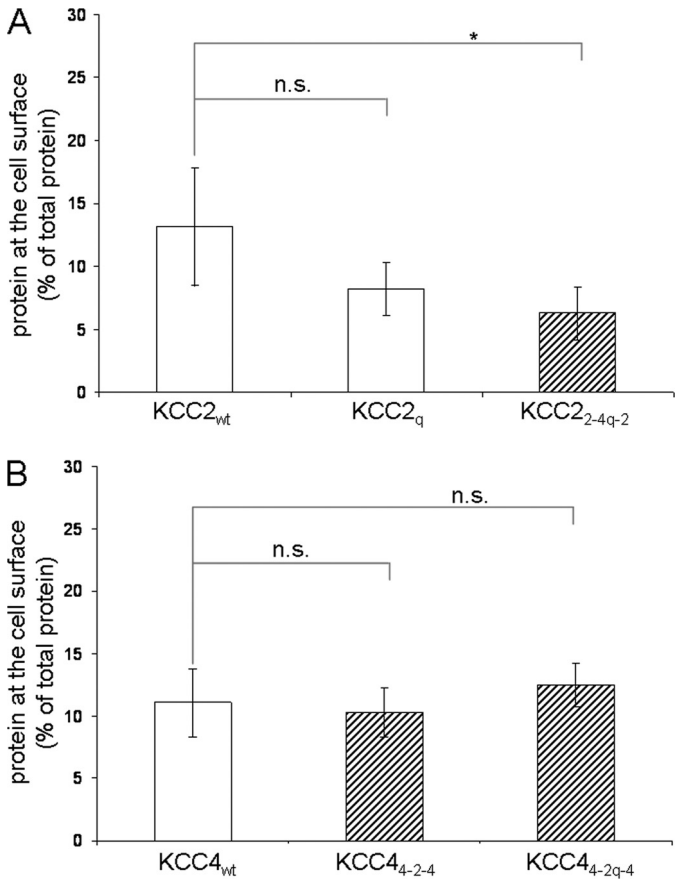

FIGURE 8. **Cell surface expression of transport-inactive cysteine mutants.** Transfected cells were labeled with sulfosuccinimidyl 2-(biotinamido)-ethyl-1,3-dithiopropionate. The cell surface amount of the indicated proteins was measured by quantifying the eluate by immunoblot analysis. *A*, $KCC2_{wt}$ and $KCC2_q$ are at similar levels at the surface, whereas $KCC2_{2-4q-2}$ was decreased at the surface compared with $KCC2_{wt}$ ($p = 0.021$). *B*, $KCC4_{wt}$ and the two transport-inactive chimeras $KCC4_{4-2-4}$ and $KCC4_{4-2q-4}$ are equally expressed at the cell surface. The plot depicts the mean of four experiments ± S.D. (*error bars*). *, $p < 0.05$; *n.s.*, not significant.

was closer to that of KCC4 than to KCC2 (Fig. 7). This indicates but does not prove that the LEL plays a role in the affinity for loop diuretics and is probably involved in binding. Unfortunately, the strongly reduced or completely abolished transport activity in other chimeras prevented analyzing their furosemide sensitivity. A previous analysis in the related NKCC1 failed to identify the bumetanide-binding site but did not analyze the LEL separately (41). In this study, nonlinear effects were observed in the analyzed NKCC1 chimera, and the authors therefore concluded that multiple sites affect binding of loop diuretics. This is in agreement with our observation that the IC_{50} of the chimera $KCC2_{2\text{-}4\text{-}2}$ was not congruent with that of $KCC4_{wt}$.

In summary, our data reveal an important role of the LEL on the transport-active conformation of KCC2 and KCC4. Furthermore, our study demonstrates a robust difference in the LEL of KCC2 and KCC4, a region so far not presumed to participate in the different functional properties of these two cotransporters. This will open up new avenues in structure-function analysis of KCCs, and future studies will reveal whether this difference relates not only to a different affinity to loop diuretics but also to other differences, such as the activity under isotonic conditions.

Acknowledgments—We gratefully acknowledge Martina Reents and Kornelia Ociepka for superb technical support, Jessica Nägele and Anne Ripperger for help in the generation of some constructs, and Jens Schindler for helpful discussions and advice concerning some of the experiments.

REFERENCES

1. Rivera, C., Voipio, J., Payne, J. A., Ruusuvuori, E., Lahtinen, H., Lamsa, K., Pirvola, U., Saarma, M., and Kaila, K. (1999) *Nature* **397,** 251–255
2. Hübner, C. A., Stein, V., Hermans-Borgmeyer, I., Meyer, T., Ballanyi, K., and Jentsch, T. J. (2001) *Neuron* **30,** 515–524
3. Balakrishnan, V., Becker, M., Löhrke, S., Nothwang, H. G., Güresir, E., and Friauf, E. (2003) *J. Neurosci.* **23,** 4134–4145
4. Tanis, J. E., Bellemer, A., Moresco, J. J., Forbush, B., and Koelle, M. R. (2009) *J. Neurosci.* **29,** 9943–9954
5. Reynolds, A., Brustein, E., Liao, M., Mercado, A., Babilonia, E., Mount, D. B., and Drapeau, P. (2008) *J. Neurosci.* **28,** 1588–1597
6. Woo, N. S., Lu, J., England, R., McClellan, R., Dufour, S., Mount, D. B., Deutch, A. Y., Lovinger, D. M., and Delpire, E. (2002) *Hippocampus* **12,** 258–268
7. Hershfinkel, M., Kandler, K., Knoch, M. E., Dagan-Rabin, M., Aras, M. A., Abramovitch-Dahan, C., Sekler, I., and Aizenman, E. (2009) *Nat. Neurosci.* **12,** 725–727
8. Hewitt, S. A., Wamsteeker, J. I., Kurz, E. U., and Bains, J. S. (2009) *Nat. Neurosci.* **12,** 438–443
9. Coull, J. A., Boudreau, D., Bachand, K., Prescott, S. A., Nault, F., Sík, A., De Koninck, P., and De Koninck, Y. (2003) *Nature* **424,** 938–942
10. Howard, H. C., Mount, D. B., Rochefort, D., Byun, N., Dupré, N., Lu, J., Fan, X., Song, L., Rivière, J. B., Prévost, C., Horst, J., Simonati, A., Lemcke, B., Welch, R., England, R., Zhan, F. Q., Mercado, A., Siesser, W. B., George, A. L., Jr., McDonald, M. P., Bouchard, J. P., Mathieu, J., Delpire, E., and Rouleau, G. A. (2002) *Nat. Genet.* **32,** 384–392
11. Boettger, T., Rust, M. B., Maier, H., Seidenbecher, T., Schweizer, M., Keating, D. J., Faulhaber, J., Ehmke, H., Pfeffer, C., Scheel, O., Lemcke, B., Horst, J., Leuwer, R., Pape, H. C., Völkl, H., Hübner, C. A., and Jentsch, T. J. (2003) *EMBO J.* **22,** 5422–5434
12. Boettger, T., Hübner, C. A., Maier, H., Rust, M. B., Beck, F. X., and Jentsch, T. J. (2002) *Nature* **416,** 874–878
13. Gamba, G. (2005) *Physiol. Rev.* **85,** 423–493
14. Payne, J. A., Stevenson, T. J., and Donaldson, L. F. (1996) *J. Biol. Chem.* **271,** 16245–16252
15. Mount, D. B., Mercado, A., Song, L., Xu, J., George, A. L., Jr., Delpire, E., and Gamba, G. (1999) *J. Biol. Chem.* **274,** 16355–16362
16. Casula, S., Shmukler, B. E., Wilhelm, S., Stuart-Tilley, A. K., Su, W., Chernova, M. N., Brugnara, C., and Alper, S. L. (2001) *J. Biol. Chem.* **276,** 41870–41878
17. Blaesse, P., Guillemin, I., Schindler, J., Schweizer, M., Delpire, E., Khiroug, L., Friauf, E., and Nothwang, H. G. (2006) *J. Neurosci.* **26,** 10407–10419
18. Uvarov, P., Ludwig, A., Markkanen, M., Soni, S., Hübner, C. A., Rivera, C., and Airaksinen, M. S. (2009) *J. Biol. Chem.* **284,** 13696–13704
19. Simard, C. F., Bergeron, M. J., Frenette-Cotton, R., Carpentier, G. A., Pelchat, M. E., Caron, L., and Isenring, P. (2007) *J. Biol. Chem.* **282,** 18083–18093
20. Casula, S., Zolotarev, A. S., Stuart-Tilley, A. K., Wilhelm, S., Shmukler, B. E., Brugnara, C., and Alper, S. L. (2009) *Blood Cells Mol. Dis.* **42,** 233–240
21. Strange, K., Singer, T. D., Morrison, R., and Delpire, E. (2000) *Am. J. Physiol. Cell Physiol.* **279,** C860–C867
22. Rinehart, J., Maksimova, Y. D., Tanis, J. E., Stone, K. L., Hodson, C. A., Zhang, J., Risinger, M., Pan, W., Wu, D., Colangelo, C. M., Forbush, B., Joiner, C. H., Gulcicek, E. E., Gallagher, P. G., and Lifton, R. P. (2009) *Cell* **138,** 525–536
23. Payne, J. A. (1997) *Am. J. Physiol.* **273,** C1516–C1525
24. Mercado, A., Song, L., Vazquez, N., Mount, D. B., and Gamba, G. (2000) *J. Biol. Chem.* **275,** 30326–30334
25. Song, L., Mercado, A., Vázquez, N., Xie, Q., Desai, R., George, A. L., Jr., Gamba, G., and Mount, D. B. (2002) *Mol. Brain Res.* **103,** 91–105
26. Mercado, A., Broumand, V., Zandi-Nejad, K., Enck, A. H., and Mount, D. B. (2006) *J. Biol. Chem.* **281,** 1016–1026
27. Bergeron, M. J., Gagnon, E., Caron, L., and Isenring, P. (2006) *J. Biol. Chem.* **281,** 15959–15969
28. Kirsch, R. D., and Joly, E. (1998) *Nucleic Acids Res.* **26,** 1848–1850
29. Delpire, E., Days, E., Lewis, L. M., Mi, D., Kim, K., Lindsley, C. W., and Weaver, C. D. (2009) *Proc. Natl. Acad. Sci. U.S.A.* **106,** 5383–5388
30. Karadsheh, M. F., Byun, N., Mount, D. B., and Delpire, E. (2004) *Neuroscience* **123,** 381–391
31. Gerelsaikhan, T., and Turner, R. J. (2000) *J. Biol. Chem.* **275,** 40471–40477
32. Uvarov, P., Ludwig, A., Markkanen, M., Pruunsild, P., Kaila, K., Delpire, E., Timmusk, T., Rivera, C., and Airaksinen, M. S. (2007) *J. Biol. Chem.* **282,** 30570–30576
33. Gagnon, K. B., England, R., and Delpire, E. (2006) *Mol. Cell Biol.* **26,** 689–698
34. Hartmann, A. M., Blaesse, P., Kranz, T., Wenz, M., Schindler, J., Kaila, K., Friauf, E., and Nothwang, H. G. (2009) *J. Neurochem.* **111,** 321–331
35. Henriksen, U., Fog, J. U., Litman, T., and Gether, U. (2005) *J. Biol. Chem.* **280,** 36926–36934
36. Adragna, N. C., Di Fulvio, M., and Lauf, P. K. (2004) *J. Membr. Biol.* **201,** 109–137
37. Jacoby, S. C., Gagnon, E., Caron, L., Chang, J., and Isenring, P. (1999) *Am. J. Physiol.* **277,** C684–C692
38. Saeki, T., Kuroda, T., Matsumoto, M., Kanamoto, R., and Iwami, K. (2002) *Biosci. Biotechnol. Biochem.* **66,** 467–470
39. Martinez, G. Q., and Maduke, M. (2008) *PLoS One* **3,** e2746
40. Ellgaard, L., and Helenius, A. (2003) *Nat. Rev. Mol. Cell Biol.* **4,** 181–191
41. Isenring, P., Jacoby, S. C., Chang, J., and Forbush, B. (1998) *J. Gen. Physiol.* **112,** 549–558